Compact High Gain Microstrip Array Antenna Using DGS Structure for 5G Applications

Hesham M. Emara[1, *], Sherif K. El Dyasti[1], Hussein H. M. Ghouz[1], Mohamed Fathy Abo Sree[1], and Sara Y. Abdel Fatah[2, 3]

Abstract—In this paper, a microstrip millimeter-wave (MMW) array antenna with a defected ground structure (DGS) has been presented for the applications of fifth generation (5G) wireless networks. This novel antenna, which has small dimensions with higher gain, can be used for licensed 5G applications in many countries, like the United States of America, Canada, Australia, Japan, India, and China. It also covers a band that is planned for licensed use in some countries, like Colombia and Mexico. The proposed model has a single element design, and for gain and efficiency enhancement, a two-element array has been designed. Both single and two element models resonate at a frequency of 39.96 GHz. Using a commercial electromagnetic simulator (CST-Studio), the model was designed and optimized with the goal of achieving a return loss rate of less than -10 dB. The proposed antenna is built on a compact Rogers substrate (RT-5880) with dimensions of 6 mm × 6 mm for the substrate of the single element and 9 mm × 13 mm for the two-element array. The substrate has a thickness of 0.508 mm, a dielectric constant ε_r of 2.2, and a loss tangent $\tan\delta$ value of 0.0009. This suggested design is small, low profile, and simple to guarantee the dependability, mobility, and high efficiency needed to be used with a variety of 5G wireless applications. The high gain of 11.6 dBi for the two-element array model of the proposed antenna is one of its distinctive features. The suggested single element model has an impedance bandwidth of 2.3 GHz, and 2.1 for the two-element array model, satisfying efficiency of approximately 73.5% for the single element and 85% for the two-element array model, respectively. The proposed structure, compared to other designs found in the literature, has smaller size while maintaining other parameter values of comparable orders.

1. INTRODUCTION

Millimeter-wave antenna for 5G networks has received significant attention due to the numerous needs of current and potential applications. These current and potential applications are represented by security scanners, radars, higher band 5G networks, short range wireless networks, and many other applications. 5G networks are required due to the increased use of social media, the present need for high-quality multimedia content, and the ability to handle large data rates and throughputs. The 5G technology supports data speeds that are regarded as high, ranging from 5 Gbps to 50 Gbps. Only moving from the frequency range below 28 GHz to above 28 GHz for higher 5G bandwidth from the whole MMW systems, which have frequency ranges between 3 and 300 GHz, is required to accomplish these massive bandwidths and fast data rates [1], and it is known as the millimeter wave spectrum.

Small antenna diameters with wideband and enhanced antenna beam shaping are required for 5G networks to meet their requirements. In comparison to traditional wire antennas (Yagi-Uda, helical,

* Corresponding author: Hesham Mahmoud Emara (hmemara@yahoo.com).
[1] Department of Electronics and Communications Engineering, Arab Academy for Science, Technology and Maritime Transport, Cairo, Egypt. [2] Higher Institute of Engineering and Technology, El-Tagammoe El-Khames, New Cairo, Egypt. [3] Department of Mechatronics Engineering and Automation, Faculty of Engineering, Egyptian Chinese University, Cairo, Egypt.

and spiral ones), planar multiband antenna structures like coplanar waveguide (CPW), stripline (SL), and microstrip (MS) have thus become very popular antennas [2–8]. This is because of their small size, low cost, lighter weight, and ease of installation. To attain the necessary characteristic within the MMW systems' effective working frequency, there is also a lot of interest in developing an effective microstrip patch antenna [3]. Additionally, compared to other antenna configurations, the microstrip patch antenna layout has outstanding interoperability with modern microwave circuitry and is easy to fabricate [3]. Several simulated microstrip patch antenna configurations, on the other hand, have been developed, examined, and claimed to have several wireless applications [9–11].

The model of a rectangle-shaped microstrip patch antenna, which offers greater advantages over other microstrip shapes and is simple to analyze in terms of fabrication and performance prediction, was chosen for this design [9, 10]. The proposed antenna, which is small and has a higher gain and efficiency, can be used for 5G applications in many nations according to the latest International Telecommunication Union (ITU) release, including the United States of America, Canada, China, Japan, India, and Australia [12–16]. It also covers a band that is planed for licensed use in some nations, including Colombia and Mexico [14, 15].

The researchers are facing difficulties with antenna specifications like gain and bandwidth, which are inversely correlated. As the bandwidth is increased, the gain decreases, and vice versa. The tradeoff between sizes and bandwidth, gain and bandwidth, or gain and sizes can be said to exist. As in [10] in the case of high gain, the bandwidth is poor, and the size is not as small as needed, Similarly, while the size of [9] is acceptable, the gain and bandwidth are not as important [9]. Take into account the trade-offs among bandwidth, antenna size, and gain.

Microstrip patch antennas often have two primary drawbacks: poor gain and restricted bandwidth [7–9]. As a result, some techniques for designing microstrip patches, such as tapering, insets, and DGS techniques, and ground plane reduction techniques are used for matching the impedance at a frequency radiated [17–24], are presented to allow the model to produce the best bandwidth, and are matched by the best gain in this bandwidth, as well as a compact, small antenna size. The agreement among bandwidth, gain, and efficiency with compact size is achieved in this design, and the simulation and results section demonstrates this success.

To improve the gain and bandwidth, a number of techniques such as loading of notches and slots of different shapes and sizes on the patch, posting a shorting pin on the radiating patch, and introducing a gap between patches are used for improving these parameters. The purpose of slot or notch is to reduce overall area of the patch [25].

2. DESIGN OF THE ANTENNA

The proposed antenna design was simulated on a substrate, RT Duriod 5880, with a height of 0.508 mm, and the substrate was chosen due to its mobility, accessibility, and outstanding mechanical performance.

Three models were designed in previous works in the same manner as the currently proposed single element model before the desired results of this work could be achieved. The results of the recently suggested single element model are first obtained using these three models [26], with the exception that the first model lacks the DGS and edge slots; the second model has edge slots without the DGS; and the third model has edge slots with a DGS at the ground layer [27], while the proposed single element has only insets without edge slots and DGS.

For the currently suggested single element model, Equation (14.6) in [4] is used to obtain the patch's width w_p, which is equal to 2.25 mm, and Equations (14.1), (14.2), (14.3), and (14.7) in [4] are used to obtain the patch's length l_p, which is also equal to 2.25 mm. By rolling between the values of patch width and length to achieve the required value, the patch width and length values were obtained using the prior equations in addition to the adaptive research at (CST-Studio) commercial electromagnetic simulator.

Figure 1(a) illustrates the single element design after mathematical calculations, with feedline width w_{fb} adjusted to 1.613 to achieve 50 ohm feeding port impedance Z_0 by using Equation (3.196) in [5], after making a parametric analysis for the feedline base to get the correct feedline base length l_b of 0.5 mm and feedline length l_f of 3 mm.

Since the feedline and patch have almost the same width, matched impedance may be improved by
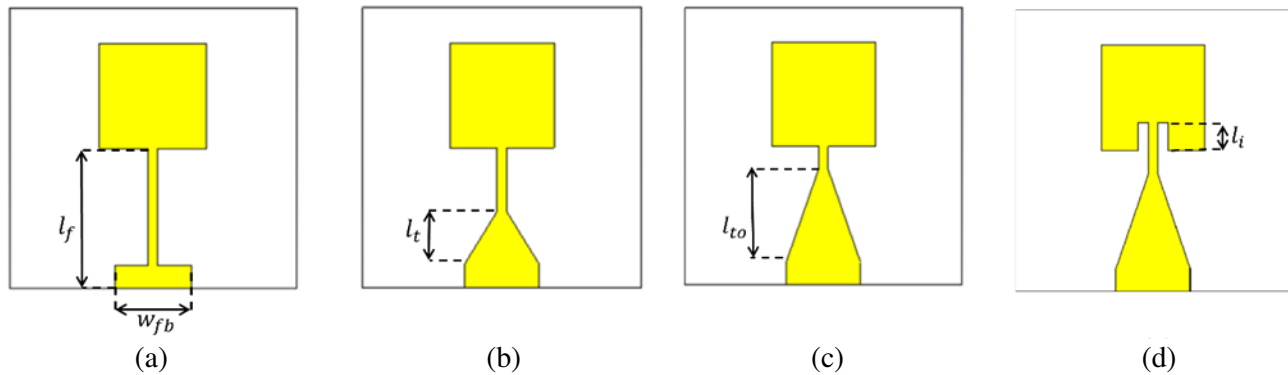
Figure 1. (a) Step one with calculated dimensions, (b) step two with tapering feedline, (c) step three after final optimization, (d) step four after adding insets with final optimization.

modifying the length of the taper connection l_t by gradually decreasing the feeding width w_{fb}, which is done by applying Equation (3.196) in [5] to have a length of tapering equal to 1.8 mm, as illustrated in Figure 1(b), and this allows the design to resonate close to the required frequency while increasing the model gain [19, 20].

Figure 1(c) depicts the improved design, which has a 2.8 mm optimum taper length. Finally, Figure 1(d) displays the complete model with two insets at the patch that resonates at the target frequency of 39.96 GHz.

2.1. Single Element Model

This model has a straightforward and compact design with feedline width w_f equal to 0.2 mm, inset length of 0.59 mm, a copper thickness of 0.035 mm, substrate dimensions of 6 mm × 6 mm, and a height of 0.508 mm.

The primary design for the single element model is depicted in Figure 2 and has a resonance frequency of 39.96 GHz, a gain of 6.4, an efficiency of 73.5%, and a bandwidth of 2.3 GHz.
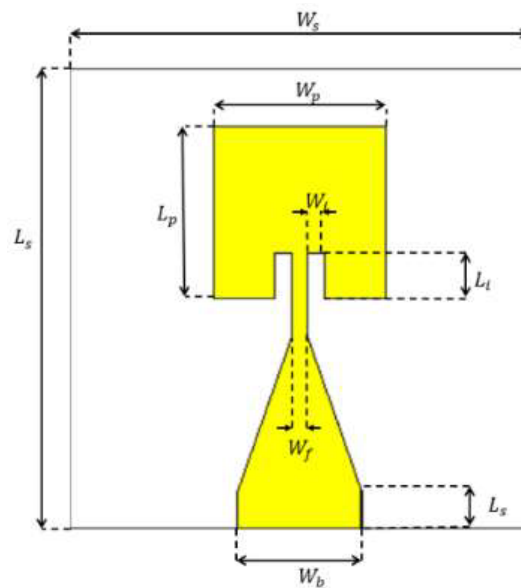

Figure 2. The geometry of the proposed single element patch.

2.2. Two-Element Microstrip Array Model

Using a corporate feed network adjusted with parametric studies, the previously proposed microstrip single element patch antenna was organized into a 2×1 array to increase radiation characteristics up to 5G specifications, as shown in Figure 3. The 50-ohm impedance feed line was configured and combined into a feed line with 100 ohm impedance, then decreased gradually by tapering the main feed line to 50 ohm. The dimensions of the two-element microstrip antenna are as in Table 1.

Table 1. Two-element array parameters.

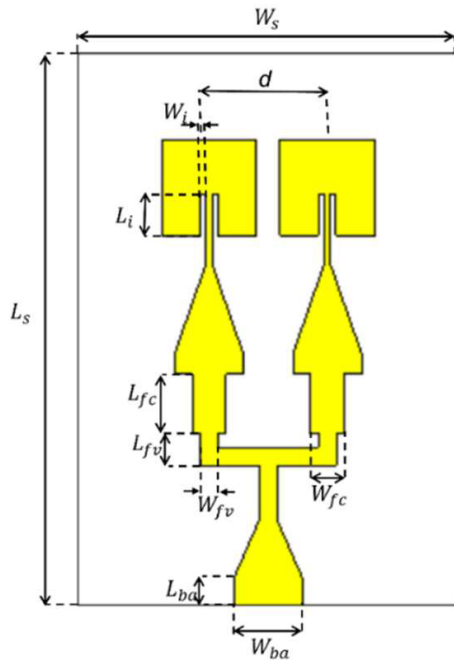| Symbol	Parameter	Dimensions (mm)
w_s	Width of the substrate	9
l_s	Length of the substrate	13
w_{ba}	Array feedline base width	1.613
l_{ba}	Array base length	0.66
w_{fv}	Vertical feedline width	0.4
l_{fv}	Vertical feedline length	0.75
w_{fc}	Vertical connection width	0.8
l_{fc}	Vertical connection length	1.4
w_i	Inset width	0.13
l_i	Inset length	0.96
d	Two patches' center distance	2.8

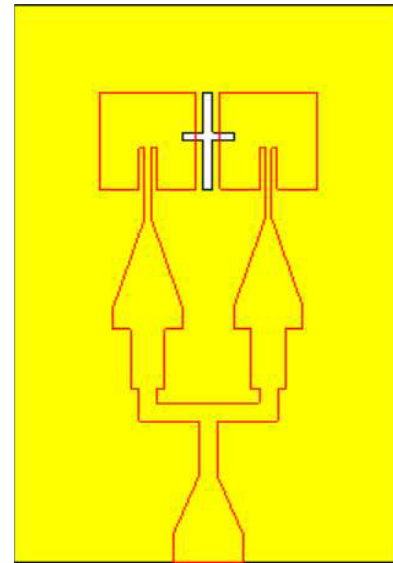**Figure 3.** The geometry of the two-element microstrip array design.

Figure 4. Back view of the proposed two-element microstrip array design.

When the gap between the centers of the two patches is more than $\frac{\lambda}{2}$, the grating lobes and mutual coupling appear, which are the model's two key design restrictions for the array, leading to the

main beam to divide into many beams. To get around these two key restrictions on the array, the distance between the centers of the two patches must be $\frac{\lambda}{2} \geq d \leq \frac{\lambda}{4}$. The computation of d took into account the air's wavelength when $\varepsilon_0 = 1$ and wavelength when $\varepsilon_r = 2.2$ at the resonance frequency of 39.96 GHz. The result was the combination of the two wavelengths divided by two, which was then used to calculate the ideal distance d. Besides distance d, the DGS is added to the ground with the help of CST to experimentally implement the DGS's dimensions and position [17, 18], which, as shown in Figure 4, has a final width of 0.2 mm, equal to 7% of d, a length of 2.27 mm for the vertical one that is almost the same as the length of the patch, and a width of 1.2 mm and a length of 0.2 mm for the horizontal one, which is positioned at the center of the patch and 10 mm from the bottom of the substrate.

The goal of the DGS is to overcome mutual coupling and get a larger bandwidth while retaining acceptable levels of efficiency and return loss [17, 18]. The DGS is used to reduce mutual coupling, allowing the frequency to precisely resonate at 39.96 GHz and improving gain. Because of this, choosing the best spacing for antenna arrays usually involves trade-offs.

3. SIMULATION AND RESULTS

The computed outcomes are bandwidth, return loss, gain, efficiency, current distribution, and radiation pattern, which are computed using a commercial electromagnetic simulator (CST-Studio).

The return loss for the designs in Figure 1 is given in Figure 5. Curves (a), (b), and (c) represent the return losses during the various optimization processes, while curve (d) represents the return losses following the final optimization.
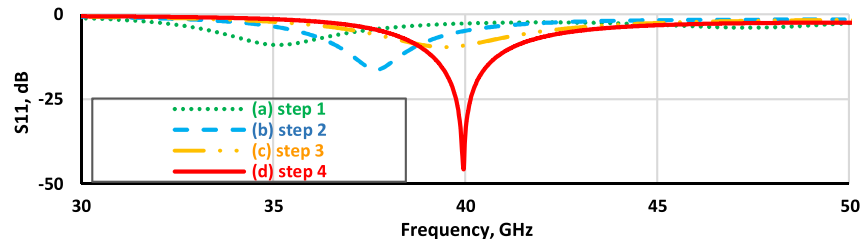

Figure 5. Return loss of the first four initial designs after optimization.

3.1. Results of the Single Element Model

Figure 6 shows the optimized results for the single antenna model in finite-difference time-domain (FDTD) and finite element method (FEM) modes for validation, and the outcomes in the two modes reveal a barely discernible difference between the two approaches, with a return loss of -45.6 dB, a gain of 6.5 dBi, a bandwidth of 2.3 GHz, and an efficiency of 73.5%. The antenna resonates at 39.96 GHz as shown in Figure 6(a).

Figure 6(b) shows the gain of the recommended antenna with a consistent directed radiation pattern. The antenna has a 6.6 dBi high gain on a single element in FDTD mode and 6.8 dBi in FEM mode, which is a very hard task that requires very careful optimization.

In Figure 6(c), the proposed model's efficiency is shown to be 73.5% at FDTD mode and 76.5% in FEM mode, which is reasonable for a single element patch antenna to have at the desired high frequency value.

Figure 7 illustrates the steady, uniform directional radiation pattern of the suggested design, which exhibits highly smooth radiation and demonstrates that all beams are equal in the same broad directional location, which indicates increasing spectral efficiency and reliable services to the subscriber and leads to covering the maximum number of subscribers at the same time in an efficient way due to its sufficient spectrum bandwidth of 2.3 GHz. Figure 7 displays the suggested antenna design's radiation pattern plots in the 39.96 GHz frequency range, and Figure 7(e) shows the current distribution along the patch and the ground at that frequency. The current is seen to be well defined around the antenna edges.
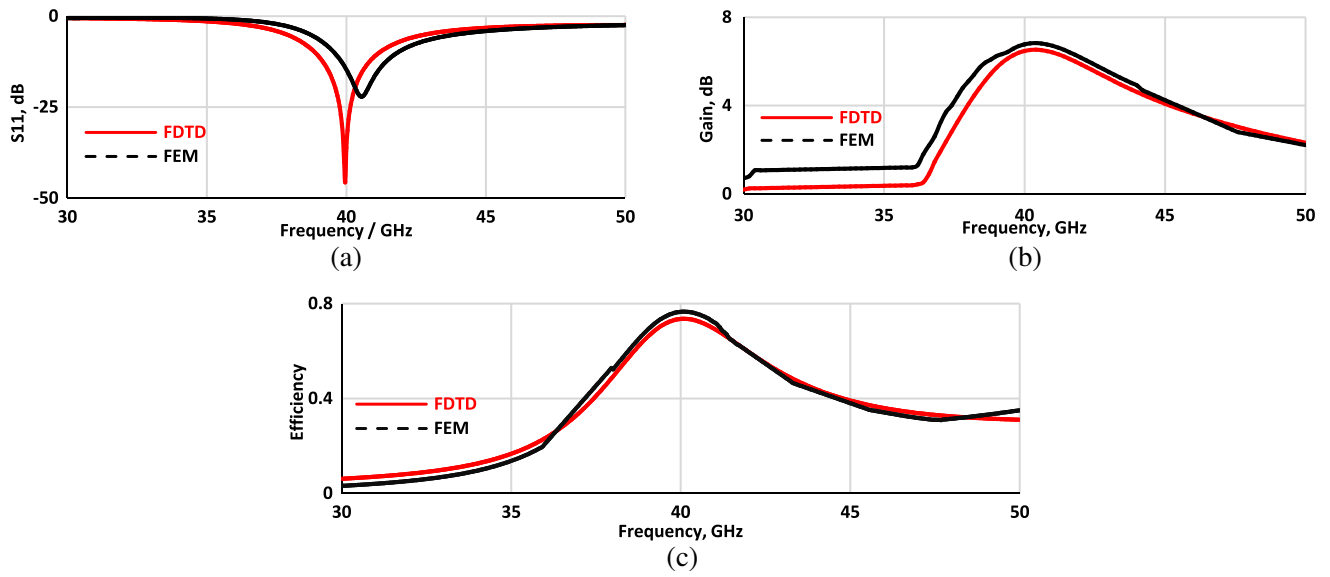
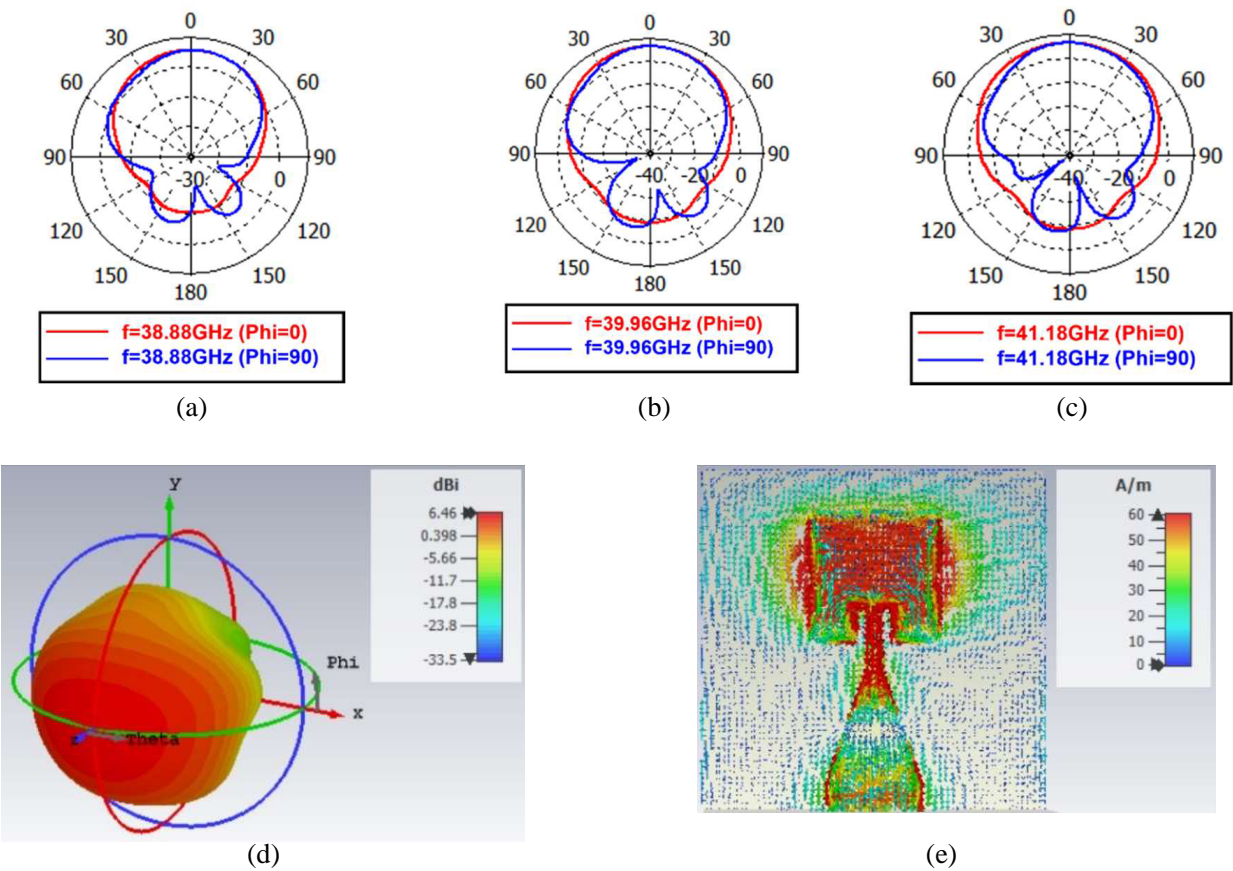**Figure 6.** (a) The optimized return loss of single element, (b) gain of the model, (c) efficiency.

Figure 7. (a), (b), and (c) are the radiation pattern of the proposed single element array model for E and H plane patterns at different frequencies. (d) The 3-D radiation pattern at 39.96 GHz. (e) Current distribution along the patch.
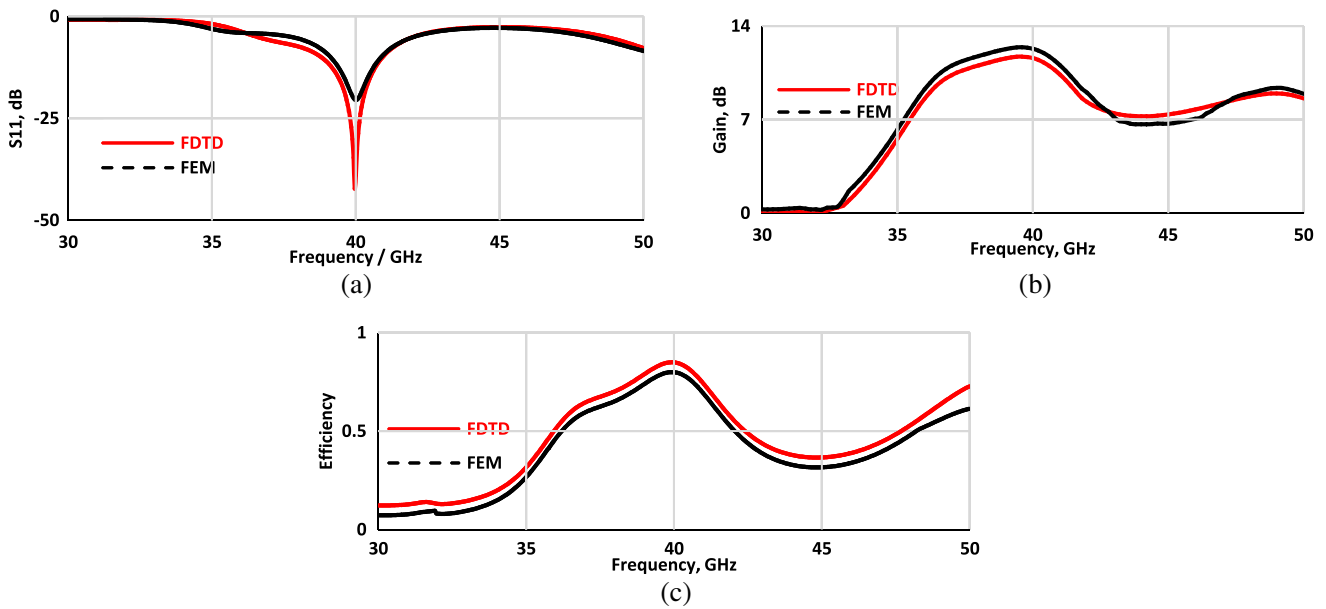
Figure 8. (a) The optimized return loss of two-element array, (b) gain of the model, (c) efficiency.

3.2. Results of the Two-Element Array Antenna

After combining the first model with a two-element microstrip array antenna to have better gain and efficiency, the array model has the same resonance frequency as the single element, which is 39.96 GHz, with a gain of 11.6 dBi, a bandwidth of 2.1 GHz, and an efficiency of 85%, as shown in Figure 8 with two simulation methods, which are FDTD and FEM modes.

Figure 8(a) shows the proposed design's optimum return loss and bandwidth. At FDTD mode, the return loss is −42 dB, and at FEM mode, it is −20.5 dB.

The proposed antenna in Figure 8(b) provides a gain of 11.6 dBi for the resonant frequency with a constant directional radiation pattern in the FDTD mode and 12.2 dBi in the FEM mode.

Figure 8(c) demonstrates the suggested model's efficiency, which is equivalent to 85% in FDTD mode and 79% in FEM mode.

The suggested design's steady, uniform directional radiation pattern displays exceptionally smooth radiation at a suitable spectrum bandwidth of 2.1 GHz. This is seen in Figure 9, where all beams are uniformly positioned in a wide directional position, suggesting enhanced spectral efficiency and stable services for the customers. Radiation pattern graphs for the recommended antenna design at 39.96 GHz are shown in Figure 9.

Because of the small dimensions of the proposed two-element array antenna, which has a width of 9 mm and length of 13 mm as mentioned previously, the measuring for this model with these dimensions was not applicable, because the 1.85 mm end-launch connector from Southwest Microwave Inc. that was used for connecting the antenna to the vector network analyzer (VNA) has a width larger than the width of the proposed antennas [28], which leads to extending the dimensions of the substrate and feedline to allow the connector to be attached to the fabricated model as shown in Table 2, taking into

Table 2. Extended size two-element parameters.

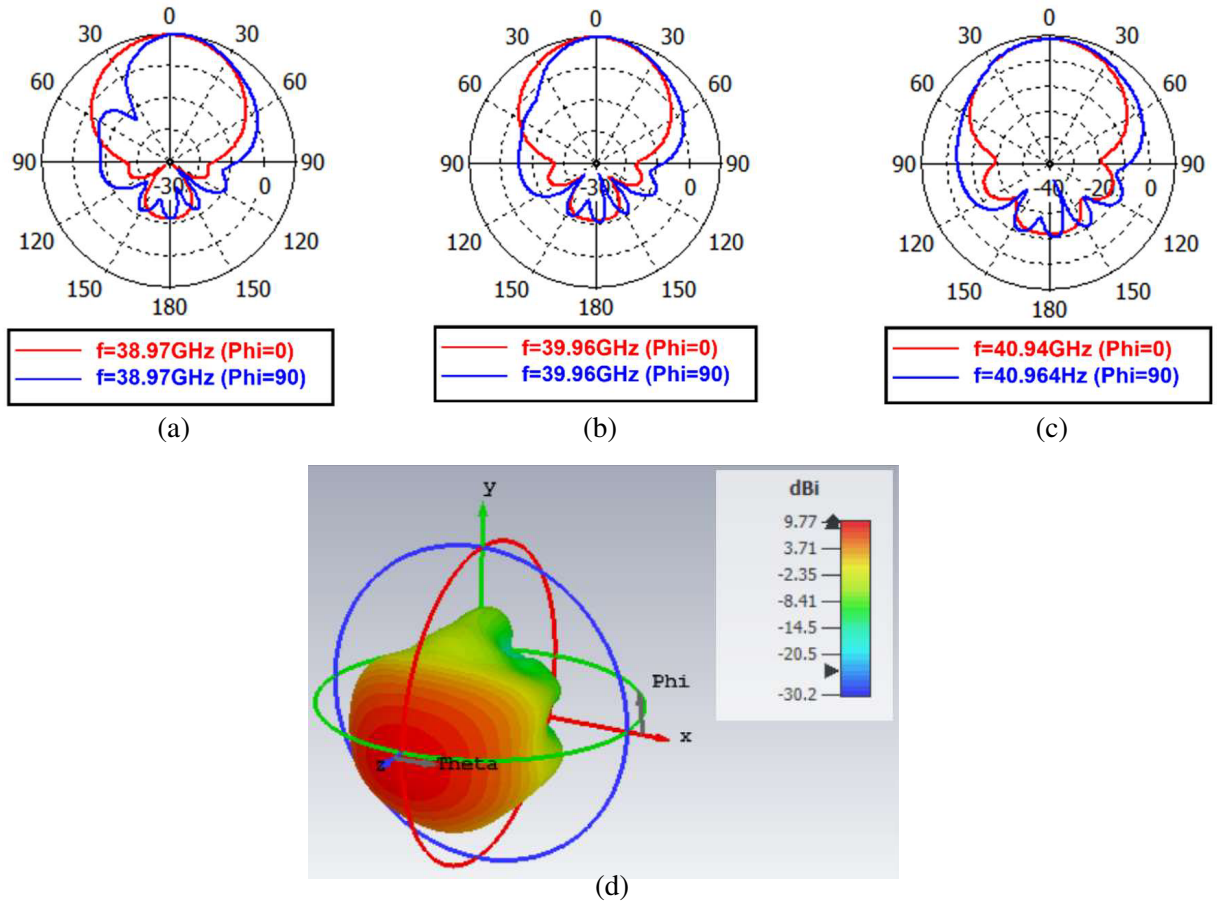| Symbol	Parameter	Dimensions (mm)
w_{es}	Width of extended substrate, & extended ground	19
l_{es}	Length of extended substrate, & extended ground	18
l_{eba}	Length of array extended base	5.66

(a)   (b)   (c)

(d)

Figure 9. The radiation pattern of the proposed two-element array model (a), (b), and (c) E and H plane patterns at different frequencies. (d) The 3-D radiation pattern at 39.96 GHz.
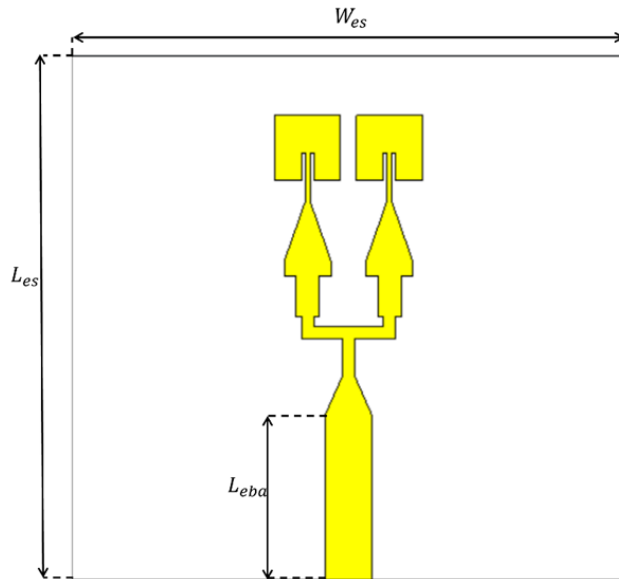

Figure 10. The geometry of the two-element antenna array after changing dimensions of substrate and feedline.
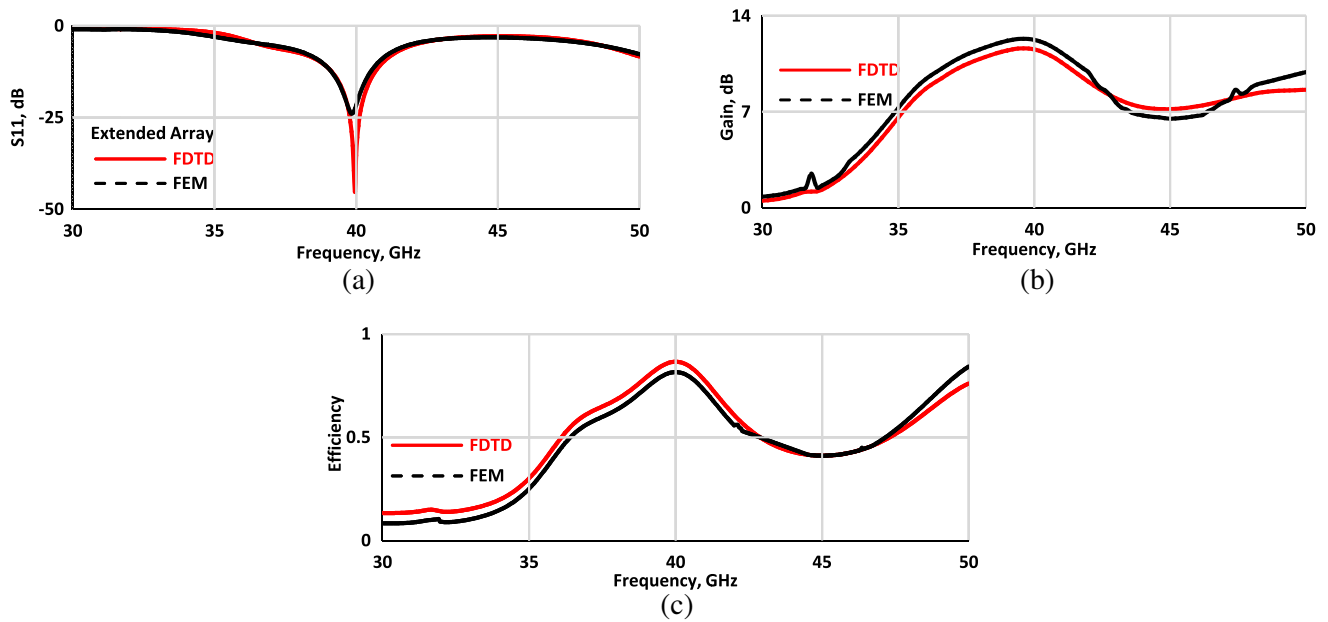
Figure 11. Optimized results of the extended size two-element model, (a) the return loss, (b) the gain of the model, and (c) efficiency.
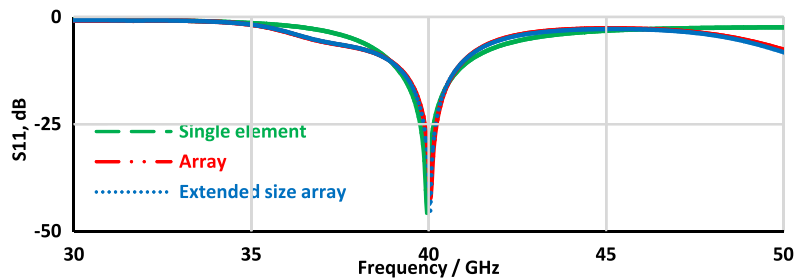
Figure 12. The return loss of the single element, two-element array, and the extended size two-element array for fabrication.

account that the result of the two-element array after having extended dimensions is the same as the optimized results of the original design.

Figure 10 shows the two-element microstrip array antenna after extending the substrate and feedline size to allow the connector to be attached to the fabricated element. Given that the extended size design yields the same outcomes as the original design, the extended size array model's resonance frequency is identical to that of the original two-element array and single element, which is 39.96 GHz with a gain of 11.6 dBi, a bandwidth of 2.1 GHz, and an efficiency of 85% as shown in Figure 11.

Figure 12 depicts the return loss of the single element, two-element array, and extended size two-element array for fabrication, as well as how extending the dimensions of the two-element model does not affect the results.

4. MEASUREMENTS OF THE RETURN LOSS

The frequency response of the return loss was measured using a VNA based on the Rhode and Schwartz model ZVA67. Southwest Microwave Inc.'s 1.85 mm end-launch connection was used to connect the antenna to the VNA. The fabricated two-element array model, which was hard to measure because of its compact size, is shown in Figure 13, while the extended two-element array model is shown in Figure 14, which is used for measurement procedures.
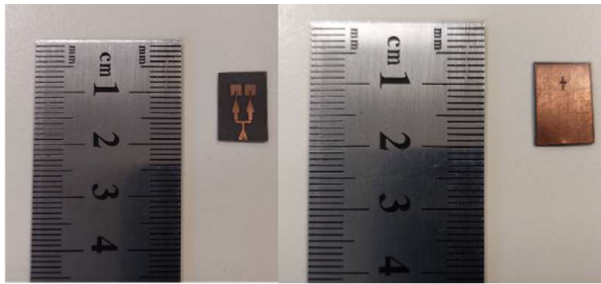
Figure 13. The front and back view of the fabricated two-element microstrip patch antenna array.
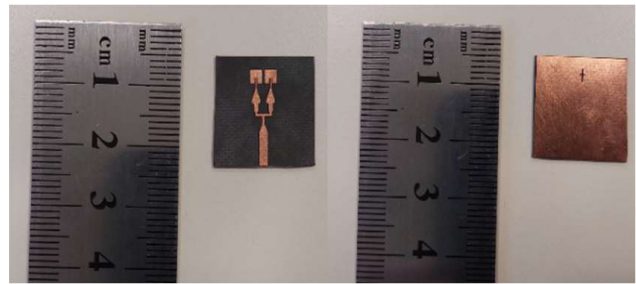

Figure 14. The front and back view of the fabricated two-element extended size microstrip patch antenna array.

After measuring the return loss of the extended model and due to limitations in measurement resources in millimeter-wave, the antenna in this band is simulated using both FDTD and FEM for the validation of the presented work. Figure 15 illustrates the frequency response of the return loss as measured by the VNA and compares it with the optimal results simulated in FDTD and FEM for the frequency of 39.96 GHz.
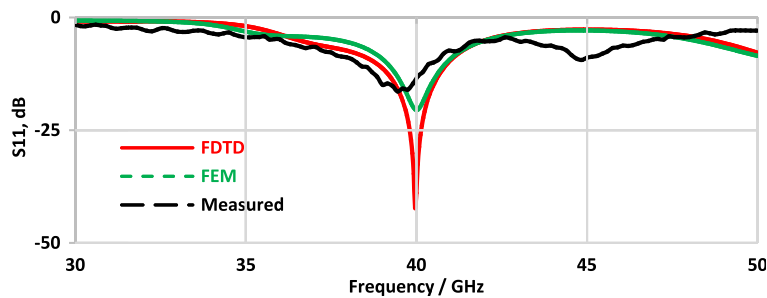

Figure 15. The simulated FDTD, FEM, and measured return loss of the two-element array.

Figure 17 depicts the actual measurement setup, and Figure 16 depicts the connector attached to the extended two-element design.
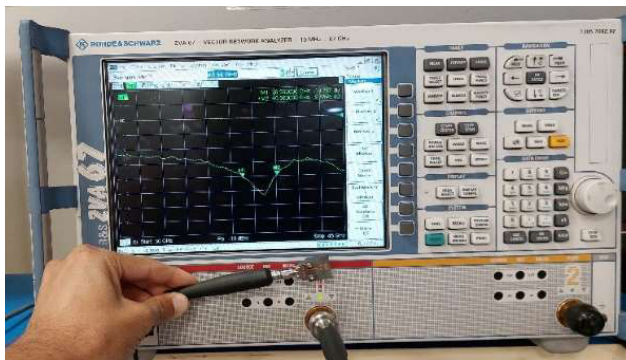

Figure 16. Measuring setup of the extended two-element array.

Figure 17. Extended two-element model attached to the connector.

Table 3. Comparison with other related works.

Ref.		Frequency GHz	Dimensions in λ^2	Bandwidth, Fractional BW [GHz-%]	Gain dBi	Efficiency	Implementation
[29]		38	3.5×3.6	2.19–5.6%	10.2	70.65%	Fabrication
[30]		34	3.5×0.8	0.92–2.6%	11.2	94.7%	CST, Fabrication
[31]		38	2.5×2.5	4.4–11.7%	8.72	NA	CST
[32]		38	2.5×2.5	0.5–1.4%	10.8	NA	HFSS, Fabrication
[33]		38	22.8×5.7	4.6–12.3%	8.4	80%	CST, Fabrication
[34]		38	22.8×5.7	1.6–4.2	8	85%	CST, Fabrication
[35]		38	3.3×1.8	2.1–5.52%	1.8	76%	HFSS, Fabrication
[36]		38	6.4×1.5	12.4–39%	9.4	92%	CST, Fabrication
Simulated results of this work	Single	39.96	0.8×0.8	2.3–5.7%	6.4	73.5	CST
	array	39.96	1.2×1.7	2.1–5.4%	11.6	85%	CST, Fabrication
	Extended array	39.96	2.5×2.4	2.1–5.4%	11.6	86.5%	CST, Fabrication

5. COMPARISON WITH RELATED WORK

To demonstrate the benefits of the suggested model for millimeter-wave applications, Table 3 compares the proposed work to the prior art to highlight the advantages of the presented model for millimeter-wave applications. In this work, the novelty of the compactness of the design and the high gain is shown in Table 3. As we observe, the dimension of the proposed two-element array model is the smallest among all reported antennas. The proposed model offers higher gain and higher efficiency than most of the reported antennas. The suggested antenna has a respectable high gain while outperforming comparable models in terms of bandwidth and compactness.

6. CONCLUSIONS

A compact size MMW high gain and high efficiency microstrip patch array antenna with DGS is presented. The design and analysis of single and two element array models are performed using an RT Duriod 5880 substrate. A tapering fed shape structure, DGS, and insets were designed to improve the gain and efficiency of the microstrip models. The gain is 6.5 for the single element and 11.6 for the two element array, which is fair enough to meet the requirements of 5G applications. The impedance bandwidth of the proposed single element model ranges from 38.9 GHz to 41.2 GHz, which is equal to 2.3 GHz, and 38.8 GHz to 40.9 GHz for the two element array model, which is equal to 2.1 GHz. In addition to the gain and bandwidth, the models satisfy an efficiency about 73.5% for the single element and 85% for the two element array model. The proposed antenna can be used for licensed 5G applications in several nations according to the latest ITU release, including America, Australia, Canada, India, Japan, and China. It also covers a band that will be utilized for licensed purposes in some nations, including Colombia and Mexico.

REFERENCES

1. Ahmad, I., H. Sun, Y. Zhang, and A. Samad, "High gain rectangular slot microstrip patch antenna for 5G mm-Wave wireless communication," *International Conference on Computer and Communication Systems (ICCCS)*, Shanghai, 2020.

2. Roh, W., J. Y. Seol, J. Park, B. Lee, J. Lee, Y. Kim, J. Cho, K. Cheun, and F. Aryanfar, "Millimeter-wave beamforming as an enabling technology for 5G cellular communications: Theoretical feasibility and prototype results," *IEEE Communications Magazine*, Vol. 52, No. 2, 106–113, 2014.

3. Ghouz, H. H., M. F. Sree, and M. A. Ibrahim, "Novel wideband microstrip monopole antenna designs for WiFi/LTE/WiMax devices," *IEEE Access*, Vol. 8, 9532–9539, 2020.

4. Balanis, C. A., *Antenna Theory: Analysis and Design*, John Wiley & Sons, 2015.

5. Pozar, D. M., *Microwave Engineering*, John Wiley & Sons, 2011.

6. Kraus, J. D. and R. J. Marhefka, *Antennas for All Applications*, John Wiley & Sons, 2002.

7. Wong, K. L., *Compact and Broadband Microstrip Antennas*, John Wiley & Sons, 2004.

8. Chen, Z. N. and M. Y. Chia, *Broadband Planar Antennas: Design and Applications*, John Wiley & Sons, 2006.

9. Al-Hetar, A. M. and E. A. Aqlan, "High performance & compact size of microstrip antenna for 5G applications," *2021 International Conference of Technology, Science and Administration (ICTSA)*, 1–3, 2021.

10. Veerendra, K., G. P. Ratna, and S. N. Bhavanam, "Design of microstrip patch antenna with parasitic elements for wideband applications," *International Journal of Innovative Research in Technology*, Vol. 6, 324–327, 2019.

11. Dheyab, E. and N. Qasem, "Design and optimization of rectangular microstrip patch array antenna using frequency selective surfaces for 60 GHz," *International Journal of Applied Engineering Research*, Vol. 11, No. 7, 4679–4687, 2016.

12. 5G Spectrum GSMA Public Policy Position. (2022). [Online]. Available: https://www.gsma.com/spectrum/wp-content/uploads/2022/06/5G-Spectrum-Positions.pdf.

13. Qualcomm, Global update on spectrum for 4G & 5G, 2020. [Online]. Available: https://www.qualcomm.com/media/documents/files/spectrum-for-4g-and-5g.pdf.

14. GTW Series. (2019). IMT in Bands Between 24.25 GHz and 86 GHz to Bolster 5G, WRC Series, WRC-19 Agenda Item 1.13. [Online]. Available: https://www.gsma.com/spectrum/wp-content/uploads/2019/07/Agenda-Item-1.13-for-5G.pdf.

15. I. Workshop, "5G and spectrum: Different approaches, iTU Work-shop: 5G and new technologies," Lome, Republic of Togo, 2019. [Online]. Available: https://www.itu.int/en/ITU-D/Regulatory-Market/Documents/Events2019/Togo/5G-Ws/Ses4_Gomes-5Gspectrum-Assignments.pdf.

16. International Telecommunication Union, Final Acts, World Radiocommunication Conference 2019 (WRC-19). [Online]. Available: https://www.itu.int/dms_pub/itu-r/opb/act/R-ACT-WRC.14-2019-PDF-E.pdf.

17. Ghouz, H. H., "Novel compact and dual-broadband microstrip MIMO antennas for wireless applications," *Progress In Electromagnetics Research B*, Vol. 63, 107–121, 2015.

18. Binshitwan, A. A., S. M. Keskeso, A. A. Alquzayzi, and A. Elbarsha, "38 GHz rectangular microstrip antenna with DGS for 5G applications," *2021 International Congress of Advanced Technology and Engineering (ICOTEN)*, 1–4, 2021.

19. Sneha, A. K., "Design of rectangular patch antenna using tapered line transfer coupled feed," *International Journal of Engineering, Management & Sciences (IJEMS)*, Vol. 1, Oct. 2014.

20. Sharma, S., C. C. Tripathi, and R. Rishi, "Impedance matching techniques for microstrip patch antenna," *Indian Journal of Science and Technology*, Vol. 10, 1–16, 2017.

21. Rahman, M. Z., K. C. Nath, and M. Mynuddin, "Performance analysis of an inset-fed circular microstrip patch antenna using different substrates by varying notch width for wireless communications," *International Journal of Electromagnetics and Applications*, Vol. 10, 19–29, 2020.

22. Prabhakar, D., P. M. Rao, and D. M. Satyanarayana, "Characteristics of patch antenna with notch gap variation for Wi-Fi application," *International Journal of Applied Engineering Research*, Vol. 11, No. 8, 5741–5746, 2016.

23. Rahman, M. Z., M. Mynuddin, and K. C. Debnath, "The significance of notch width on the performance parameters of inset feed rectangular microstrip patch antenna," *International Journal of Electromagnetics and Applications*, Vol. 10, 7–18, 2020.

24. Joshi, A. and R. Singhal, "Vertex-fed hexagonal antenna with low cross-polarization levels," *Advances in Electrical and Electronic Engineering*, Vol. 17, No. 2, 138–145, 2019.

25. Mishra, B., V. Singh, and R. Singh, "Gap coupled dual-band petal shape patch antenna for WLAN/WiMAX applications," *Advances in Electrical and Electronic Engineering*, Vol. 16, No. 2, 185, 2018.

26. Emara, H. M., H. H. Ghouz, S. K. El Dyasti, and M. F. Sree, "Novel compact microstrip antennas with two different bands for 5G applications," *2022 International Telecommunications Conference (ITC-Egypt)*, 1–6, 2022.

27. Emara, H. M., S. K. El Dyasti, H. H. Ghouz, and M. F. Sree, "Design of a compact dual-frequency microstrip antenna using DGS structure for millimeter-wave applications," *Journal of Advanced Research in Applied Sciences and Engineering Technology*, Vol. 28, No. 3, 221–234, 2022.

28. Southwest microwave, Microwave Products Division, End Launch Connectors. https://mpd.southwestmicrowave.com/product-category/end-launch-connectors/.

29. Deckmyn, T., M. Cauwe, D. V. Ginste, H. Rogier, and S. Agneessens, "Dual-band (28, 38) GHz coupled quarter-mode substrate-integrated waveguide antenna array for next-generation wireless systems," *IEEE Transactions on Antennas and Propagation*, Vol. 67, No. 4, 2405–2412, Apr. 2019.

30. Khattak, M. I., A. Sohail, U. Khan, Z. Barki, and G. Witjaksono, "Elliptical slot circular patch antenna array with dual band behaviour for future 5G mobile communication networks," *Progress In Electromagnetics Research C*, Vol. 89, 133–147, 2019.

31. Rahayu, Y. and M. I. Hidayat, "Design of 28/38 GHz dual-band triangular-shaped slot microstrip antenna array for 5G applications," *2nd International Conference on Telematics and Future Generation Networks (TAFGEN)*, 93–97, 2018.

32. Chu, H. and Y. X. Guo, "A filtering dual-polarized antenna subarray targeting for base stations in millimeter-wave 5G wireless communications," *IEEE Transactions on Components, Packaging and Manufacturing Technology*, Vol. 7, No. 6, 964–973, Jun. 2017.

33. Mahmoud, K. R. and A. M. Montaser, "Performance of tri-band multi-polarized array antenna for 5G mobile base station adopting polarization and directivity control," *IEEE Access*, Vol. 6, 8682–8694, Mar. 2018.

34. Mahmoud, K. R. and A. M. Montaser, "Synthesis of multi-polarised upside conical frustum array antenna for 5G mm-Wave base station at 28/38 GHz," *IET Microwave, Antennas and Propagation*, Vol. 12, No. 9, 1559–1569, Jul. 2018.

35. Hasan, M. N., S. Bashir, and S. Chu, "Dual band omnidirectional millimeter wave antenna for 5G communications," *Journal of Electromagnetic Waves and Applications*, Vol. 33, No. 12, 1581–1590, Aug. 2019.

36. Jilani, S. F. and A. Alomainy, "Millimetre-wave T-shaped MIMO antenna with defected ground structures for 5G cellular networks," *IET Microwaves Antennas & Propagation*, Vol. 12, No. 5, 672–677, Apr. 2018.